An extracellular protease containing a novel C-terminal extension produced by a marine-originated haloarchaeon

Dong Han[1,2], Jing Hou[1] and Heng-Lin Cui[1]*

[1]School of Food and Biological Engineering, Jiangsu University, Zhenjiang, China, [2]School of Grain Science and Technology, Jiangsu University of Science and Technology, Zhenjiang, China

Marine microorganisms have long been acknowledged as a significant reservoir of enzymes required for industrial use. In this study, a novel extracellular protease *Hsl*HlyB derived from marine-originated haloarchaeon *Halostella pelagica* DL-M4[T] was identified. *Hsl*HlyB contained polycystic kidney disease (PKD) domain and pre-peptidase C-terminal (PPC) domain at the C-terminus. Truncation and replacement of the C-terminal extension (CTE) of *Hsl*HlyB demonstrated the importance of the CTE in maintaining the protease activity secreted by haloarchaeon. *Hsl*HlyB and *Hsl*HlyBΔCTE were expressed in *Escherichia coli* BL21(DE3), and purified by high-affinity column refolding and gel filtration chromatography. The molecular masses of *Hsl*HlyB and *Hsl*HlyBΔCTE were 42 kDa and 20 kDa, respectively. The optimum catalytic reaction conditions were 50°C, pH 8.5, NaCl 3.5 M and 50°C, pH 7.5, NaCl 3 M, respectively. They showed good stability and hydrolysis capabilities towards a wide range of protein substrates. *Hsl*HlyBΔCTE showed higher catalytic reaction rate and better thermal stability than the wild type against azocasein and tetrapeptide substrate. The hydrolysates of soybean protein hydrolyzed by *Hsl*HlyBΔCTE had smaller average molecular masses and shorter average peptide chain lengths than those by *Hsl*HlyB. These results indicated the diversity of halolysins from marine-originated haloarchaea to harness organic nitrogen in the marine environment and provided promising candidates for application in various industries.

KEYWORDS

halolysin, C-terminal extension, haloarchaeon, tidal flat, marine solar salt

Introduction

It is widely recognized that marine is a reservoir of biological resources, harboring diverse microorganisms and functional enzymes. Intertidal zones with variable salinity, temperature and nutrient are kinds of important marine ecosystems including a variety of habitats, such as rocky shores, sandy beaches, soft sediments, salt marshes and mangroves

(Kon et al., 2020). Haloarchaea are the most salt-requiring and salt-resistant microorganisms partly thriving in marine salt inhabitants, such as marine solar salterns, marine lagoons and costal sediment (Lee, 2013; Cui and Dyall Smith, 2021; Sun et al., 2023). The haloarchaea that inhabit this zone have adapted to extremely harsh environments and evolved the ability to produce enzymes that function optimally in high salt concentrations, even in extreme pH and temperatures (Amoozegar et al., 2017). It is increasingly interesting to look for specific enzymes with high thermal stability, high tolerance with wide range of salinities produced by haloarchaea to meet the needs of industrial applications.

Halolysin is a kind of proteases that are secreted extracellularly by haloarchaea and exert endo-protease activity. Halolysins reported so far all belong to serine proteases with molecular masses range of 21-130 kDa (Studdert et al., 1997; Elsztein et al., 2001; Studdert et al., 2001; Elbanna et al., 2015). Halolysin plays important ecological roles in organic nitrogen degradation in saline environments and provides its host with antagonistic and defensive activities against other haloarchaea for competitive advantage (Chen et al., 2021). Halolysins were considered as excellent candidates in industries such as food production (Chaveesuk et al., 1994; Yongsawatdigul et al., 2007; Akolkar et al., 2010), cleaning agent (Jaouadi et al., 2008), peptide synthesis (Ryu et al., 1994; Ruiz et al., 2010), detergent (Akolkar et al., 2008) and waste management (Lefebvre and Moletta, 2006).

A number of halolysins have been already reported with known coding genes, including halolysins 172P1 from *Natrialba asiatica* 172P1 (Kamekura et al., 1992), R4 from *Haloferax mediterranei* R4 (Kamekura et al., 1996), SptA and SptC from *Natrinema* sp. J7 (Zhang et al., 2014; Du et al., 2015), Nep from *Natrialba magadii* (De Castro et al., 2008), HlyA from *Halococcus salifodinae* (Hou et al., 2020), Hly$_{Hap}$ from *Haladaptatus* sp. DYF46 (Hou et al., 2022). For protein domain organization, those halolysin precursors are usually made up of a Tat (twin-arginine translocation) signal peptide, an N-terminal propeptide, an S8/S53 family catalytic domain and a C-terminal extension (CTE). The CTE of halolysins are usually prepeptidase C-terminal (PPC) domain, except a combined polycystic kidney disease (PKD) domain and chitin-binding domain (ChBD) was reported in the CTE of SptC (Du et al., 2015). In recent years a marine halolysin Hly$_{Hap}$ without CTE was discovered to prefer a low salinity in contrast to most halolysins (Hou et al., 2022). CTE domains have been shown to have a significant impact on the structure and function of a protease (Gao et al., 2010), especially those secreted by the marine bacteria (Huang et al., 2017). The halolysins thus far reported are much less diverse than those of proteases from bacteria, especially halolysins of marine origin that possess ecological significance and deserve to be explored more deeply.

Strain DL-M4^T with ability of hydrolysis of gelatin and casein is the type strain of *Halostella pelagica* and was isolated from the salted seaweed produced in Dalian, Liaoning Province, China (Han and Cui, 2020). Strain DL-M4^T may originate from marine solar salt or *Laminaria* farmed in tidal zone. In this study, the potential extracellular protease genes from *Hsl. pelagica* DL-M4^T were identified, and the recombinant halolysins with different CTE domains were expressed in the heterologous host, *Haloferax*

volcanii H1424, in order to explore the effect of different CTE on *Hsl*HlyB activity. Furthermore, *Hsl*HlyB and *Hsl*HlyBΔCTE were purified and characterized to explore the diversity of the catalytic properties of halolysins and the effect of CTE on enzymatic properties. At last, the potential application of *Hsl*HlyB and *Hsl*HlyBΔCTE in hydrolysis of soybean protein under high-salt concentration were evaluated. This study would enrich our knowledge of the diversity of marine halolysins and provide a promising halophilic protease.

Materials and methods

Strains and growth conditions

Hsl. pelagica DL-M4^T (=CGMCC 1.13603^T = JCM 32954^T, GenBank accession numbers: 16S rRNA gene MH062945, genome CP040678-CP040681) with the hydrolysis ability towards casein and gelatin was isolated from the salted brown alga *Laminaria* in the previous study (Han and Cui, 2020). Other halolysin producing strains of *Hfx. mediterranei* ATCC 33500^T, *Nab. magadii* CGMCC 1.1966^T and *Hcc. salifodinae* DSM 8989^T were also used in this study. They were grown under aerobic conditions at 37°C in neutral haloarchaeal medium (NHM) (Cui et al., 2011). *Hfx. volcanii* H1424 used as the haloarchaeal host for expression was cultured in Hv-YPC medium (Stroud et al., 2012). *Escherichia coli* DH5α and BL21 (DE3) were used as host strains for cloning and protein expression, respectively. Luria-Bertani medium was used to cultivate the above *E. coli* strains at 37°C, if necessary, 100 μg mL^{-1} of ampicillin or 50 μg mL^{-1} of kanamycin was added.

In silico analysis of halolysin genes

The hmm model of Peptidase_S8 domain (Pfam accession: PF00082) was used to search for model-compatible proteins in *Hsl. pelagica* DL-M4^T via the Hmmsearch of Hmmer software (Finn et al., 2011). The protein sequence of Nep from *Nab. magadii* (accession no. AAV66536) was also used to find halolysin genes in the genome of *Hsl. pelagica* DL-M4^T by BlastP tool (Altschul et al., 1997). The resulting potential halolysins were also confirmed against Swiss-Prot databases. The theoretical molecular mass and isoelectric point were predicted using Prot Param (https://web.expasy.org/protparam/). Signal peptide prediction was performed using SignalP 5.0 (Armenteros et al., 2019). Protein domain prediction was performed using InterProScan (Quevillon et al., 2005). The C-terminal domain structure was modelled by SWISS-MODEL Workspace (https://swissmodel.expasy.org/). The structure of *Hsl*HlyB was predicted by AlphaFold2 (Jumper et al., 2021).

Vector construction

Three potential halolysin genes and *Hsl*HlyB without CTE or PKD domain encoding genes were amplified by PCR using *Hsl.*

pelagica DL-M4^T genomic DNA as the template. The encoding genes for chimeras of *Hsl*HlyB with different CTE domains were obtained using the overlapping extension PCR method as described previously (Hou et al., 2020) using *Hsl. pelagica* DL-M4^T, *Hfx. mediterranei* ATCC 33500^T, *Nab. magadii* CGMCC 1.1966 and *Hcc. salifodinae* DSM 8989^T genomic DNA as the template. The PCR amplification was performed using the KOD-plus-neo DNA polymerase (Toyobo), and primer pairs shown in Table S1. The products were digested with a pUCm-T vector using *Eco*RI, *Bam*HI/*Sph*I or *Nco*I, *Xho*I as the restriction enzyme sites (the restriction endonucleases used for corresponding genes shown in Table S1). The purified amplicons of potential halolysin genes and encoding genes of *Hsl*HlyB variants were cloned into the haloarchaeal shuttle vector pTA under the strong promoter P.*phaR* (Liu et al., 2015) for expression in *Hfx. volcanii*. The purified amplicons of *HslHlyB* and *HslHlyBΔCTE* were cloned into the vector pET28a under *Lac* promoter for expression in *E. coli* BL21 (DE3). The colony PCR and Sanger sequencing were used to verify the inserts in the constructed plasmids.

Expression and purification of halolysins

There were two kinds of expressing hosts used in this study. For expressing *Hsl*HlyA, *Hsl*HlyB, *Hsl*HlyC and *Hsl*HlyB variants, the expression plasmid was transformed into *Hfx. volcanii* H1424. Cell cultures were grown in Hv-YPC medium at 37°C until the stationary phase. Culture supernatant (12,000 g, 10 min, 4°C) was used as the crude enzyme to assay the extracellular protease activity. To obtain purified enzymes, the *Hsl*HlyB and *Hsl*HlyBΔCTE precursors were expressed in *E. coli* BL21 (DE3) and *in vitro* refolded as previously described (Hou et al., 2021; Hou et al., 2022). For *in vitro* refolding, the recombinant cells were firstly resuspended in lysis buffer (8 M urea, 10 mM CaCl$_2$, 50 mM Tris-HCl, 2 mM β-mercaptoethanol, pH 8.0). After sonicating and centrifuging, the supernatant containing denatured precursors was loaded onto the 2 mL Ni-column, then washed with lysis buffer containing 40 mM imidazole. The Ni-column bound precursors were incubated in refolding buffer (4 M NaCl, 10 mM CaCl$_2$, 50 mM Tris-HCl, pH 8.0) for 24 h at 37°C to fully refold. After washing with the refolding buffer containing 20 mM imidazole, the target proteins were eluted using the refolding buffer containing 100 mM imidazole. The refolded halolysins were further purified by molecular sieves using the Superdex 200 10/300 GL column (GE healthcare).

Functional screening of potential halolysins and *Hsl*HlyB mutants for hydrolytic activities

The Hv-YPC agar plates added with 0.5% (w/v) skim milk or gelatin were used to evaluate the protein hydrolysis capacity of the recombinant haloarchaeal cells (inoculation amount: 5 µL). The plates were incubated at 37°C for 14 days for activity verification.

Frazier's reagent (g/L: HgCl$_2$, 150 g; concentrated HCl, 200 mL) was used to detect the hydrolysis of gelatin.

Enzyme activity assay

Enzyme activity towards azocasein (Sigma-Aldrich, USA) and N-Succinyl-Ala-Ala-Pro-Phe p-nitroanilide (Suc-AAPF-pNA, Sigma-Aldrich, USA) was determined as previously described (Hou et al., 2021). For determination of azocaseinolytic activity, 250 µL of crude enzyme was reacted with an equal volume of 0.5% azocasein (buffer: 2 M NaCl, 50 mM Tris-HCl, pH 8.0) at 37°C for 1 h. The reaction was terminated by the addition of 500 µL of 10% TCA, left at room temperature for 15 min and then centrifuged at 10,000 g for 10 min. 300 µL of supernatant was added to an equal volume of 1 M NaOH, and then centrifuged to remove the precipitate. The absorbance of the supernatant at 440 nm (A$_{440}$) was recorded. In the control experiments, solutions of the enzyme and substrate were incubated separately. Under specific reaction conditions the amount of enzyme required to increase OD$_{440}$ by 0.01 was defined as 1 unit of enzyme activity. When purified enzyme was used for azocaseinolytic activity assay, 10 µg of enzyme was used in each reaction. For the enzyme activity towards Suc-AAPF-pNA, 300 µL of crude enzyme was mixed with 300 µL of Suc-AAPF-pNA (0.4 mM) in the buffer of 2 M NaCl, 50 mM Tris HCl (pH 8.0). The initial hydrolysis rate of the tetrapeptide substrate was measured at 410 nm using a DU800 Nucleic Acid Protein Analyzer with the temperature controlled at 37°C. One unit of protease activity (U) was defined as the amount of enzyme required to produce 1 µmol pNa (extinction coefficient of 8,480 M^{-1}cm^{-1}) per minute under certain conditions. Protein concentration was measured by Bradford assay (Beyotime Institute of Biotechnology, China) (Bradford, 1976).

Effect of temperature, pH and salinity on protease activities

To determine the optimal reaction temperature, protease activities were measured at temperatures of 20°C, 30°C, 35°C, 40°C, 45°C, 50°C, 55°C, 60°C and 65°C, respectively, in 2 M NaCl, 50 mM Tris-HCl (pH 8.0). Thermal stability was determined by pre-incubation of the enzyme at 30°C, 40°C, 50°C and 60°C for 0 min, 20 min, 40 min and 60 min, respectively. Then the protease activity was measured at optimum temperature.

The optimal pH was determined by assaying protease activities at the optimum temperature and 2 M NaCl in different buffers of 50 mM K$_2$HPO$_4$/KH$_2$PO$_4$ buffer at pH 6.0, pH 6.5, pH 7.0 and pH 7.5; 50 mM Tris-HCl buffer at pH 7.5, pH 8.0, pH 8.5 and pH 9.0; 50 mM CHES-NaOH buffer at pH 9.0, pH 10.0 and pH 10.5. pH stability was determined by pre-incubation of the enzyme at room temperature at pH 6.0 (50 mM K$_2$HPO$_4$/KH$_2$PO$_4$ buffer), pH 8.0 (50 mM Tris-HCl buffer) and pH 10.0 (50 mM CHES-NaOH buffer) for 0 min, 20 min, 40 min and 60 min, respectively. Then the protease activity was measured at the optimum temperature.

The optimal NaCl concentration was determined by assaying at NaCl concentrations of 0.4 M, 0.5 M, 1.0 M, 1.5 M, 2.0 M, 2.5 M, 3.0 M, 3.5 M and 4.0 M, respectively, at the optimum pH and temperature. Salinity stability was determined by pre-incubation of the enzyme at room temperature with 0 M, 2 M and 4 M NaCl for 0 min, 20 min, 40 min and 60 min, respectively. Then the protease activity was measured at the optimum reaction condition.

Effect of different compounds on protease activities

The protease activities were measured with additives of 5 mM of metal ions or 5% (v/v) of organic solvents or 10% (v/v) of detergents. The protease inhibitors included 4 mM phenylmethylsulfonyl fluoride (PMSF), 10 mM pepsin inhibitor (Pepstatin A), 1 mM p-chloromercuribenzoate (PCMB), 10 mM dithiothreitol (DTT) and 5 mM ethylene diamine tetraacetic acid (EDTA). The protease activities were measured at their respective optimal conditions (3.5 M NaCl, 50°C, pH 8.5 for HslHlyB and 3 M NaCl, 50°C, pH 7.5 for HslHlyBΔCTE).

Hydrolysis of different protein substrates

The enzyme activity (in terms of tyrosine produced) was determined by reacting with azocasein, casein, gelatin, bovine serum protein, bovine hemoglobin, egg albumin, fish collagen or skim milk at a final concentration of 5 g/L under their respective optimal conditions (3.5 M NaCl, 50°C, pH 8.5 for HslHlyB and 3 M NaCl, 50°C, pH 7.5 for HslHlyBΔCTE).

Determination of K_m and V_{max}

The kinetic parameters of the purified halolysins were determined against 0.01-9.44 mM azocasein or 0.01-2 mM Suc-AAPF-pNA. The reaction with 0.8 μg protease was performed at the optimal conditions. The K_m and V_{max} values were calculated from the Michaelis-Menten equation by nonlinear regression (GraphPad Prism 7).

Sodium dodecyl sulphate–polyacrylamide gel electrophoresis analysis

Tris-glycine SDS-PAGE was performed according to the method of King and Laemmli (King and Laemmli, 1971). To prevent the self-degradation of halolysin during the sample pretreatment, TCA-acetone precipitation was used to denature halolysin, referring to Hou's method (Hou et al., 2021). After that, 20-40 μL of loading buffer containing 8 M urea was added to the protein precipitate with DTT at a final concentration of 100 mM, and the supernatant was used for SDS-PAGE analysis.

Protein sequencing and molecular mass determination

After tris-glycine SDS-PAGE analysis, the protein bands were in-gel digested as described by Shevchenko (Shevchenko et al., 1996), and the tryptic peptides were sequenced using Matrix-Assisted Laser Desorption Ionization Time of Flight/Time of Flight Mass Spectrometry (MALDI-TOF/TOF MS) (AB Sciex 5800, USA). The molecular mass of the mature halolysin was determined by gel filtration chromatography as previously described (Hou et al., 2021).

Mass spectrometry analysis of the soybean protein isolate hydrolysates

Soybean protein isolate (Sinopharm) was washed three times with sterile distilled water to remove soluble peptides. The reaction with 0.1 mg/mL enzyme and 5% (m/v) soybean protein isolate was carried out under optimum reaction conditions (3.5 M NaCl, 50°C, pH 8.5 for HslHlyB and 3 M NaCl, 50°C, pH 7.5 for HslHlyBΔCTE) for 24 h. The enzyme was inactivated in boiling water bath for 10 min. The protein hydrolysate solution was filtered, then desalted by a C18 column and identified by LC-MS (Agilent 1260/6460 LC/Triple Quadrupole MS).

Results and discussion

Identification of potential halolysin genes from *Hsl. pelagica* DL-M4[T]

Hmmer is a sensitive search tool for searching homologs protein by using hidden Markov models. The Pfam hmm model of Peptidase_S8 domain was used to search for potential halolysin genes. Nep, a most intensively-studied halolysin from *Nab. magadii* (De Castro et al., 2008), was also used to search for potential halolysin by BlastP tool. Three potential halolysins HslHlyA, HslHlyB and HslHlyC were found, with 24.5-56.0% identities to Nep (Table S2). Their amino acid sequences were compared against the SwissProt database. The most similar protein for HslHlyA was found to be SubE, the Bacillus subtilis protease, from *Bacillus licheniformis*, with 37.8% amino acid identity; the most similar proteins for HslHlyB and HslHlyC were halolysin from *Hfx. mediterranei* R4, with amino acid identities of 57.4% and 23.9%, respectively. The theoretical molecular masses of HslHlyA (383 aa), HslHlyB (613 aa) and HslHlyC (488 aa) were 39.5, 63.0 and 51.2 kDa and pI values of 4.20, 4.06 and 4.30, respectively. All of them contained Tat signal peptide and S8/S53 peptidase catalytic domain with aspartate-histidine-serine catalytic active sites. HslHlyA and HslHlyC did not contain any CTE while HslHlyB was found to contain two domains, PKD domain and PPC domain, at the C-terminus. SWISS-MODEL homology modeling was used to predict the secondary structure of PKD and PPC domains of HslHlyB, and found that they both have seven β-sheets (Figure S1). The structure

of *Hsl*HlyB was determined with molecular replacement using a model obtained from Alphafold2 (the predicted local distance difference test score is 87.4). The 3D structure shows that *Hsl*HlyB consists of 4 domains, with 2 independent β-sandwich structures at the C-terminus (Figure S1). Some proteases distributed in different families contain CTEs, such as PKD domain, PPC domain and ChBD domain (Huang et al., 2017). These domains are different in amino acid sequences and also structures (Huang et al., 2019). But they are all rich in β-sheets (Huang et al., 2017). There are several studies on CTE function of bacterial proteases (Wang et al., 2010; He et al., 2012), but few studies on CTE of haloarchaeal proteases (Xu et al., 2011; Marem et al., 2018).

The potential halolysin genes were expressed in the non-extracellular protease-producing *Hfx. volcanii* H1424, a halophilic archaeal host, to investigate whether the encoded protein was active. Only the recombinant strain expressing *Hsl*HlyB showed significant hydrolysis zones on milk and gelatin plates, those expressing *Hsl*HlyA or *Hsl*HlyC could not hydrolyze milk or gelatin (Figures 1A, B). Meanwhile, the extracellular supernatant of the recombinant strain with *Hsl*HlyB had the ability to hydrolyze azocasein and Suc-AAPF-pNA, that of *Hsl*HlyA could weekly hydrolyze Suc-AAPF-pNA but not azocasein, and that of *Hsl*HlyC could not hydrolyze azocasein or Suc-AAPF-pNA (Figure 1C). According to these results, *Hsl*HlyB has low sequence similarity to other reported proteases (with the highest identity of 57.4% in SwissProt database) and ability to hydrolyze milk, gelatin, azocasein and tetra-peptide substrate. To our knowledge, no halolysin from the genus *Halostella* has been characterized. Additionally, this is the first reported halolysin with PKD and PPC domains at the C-terminus.
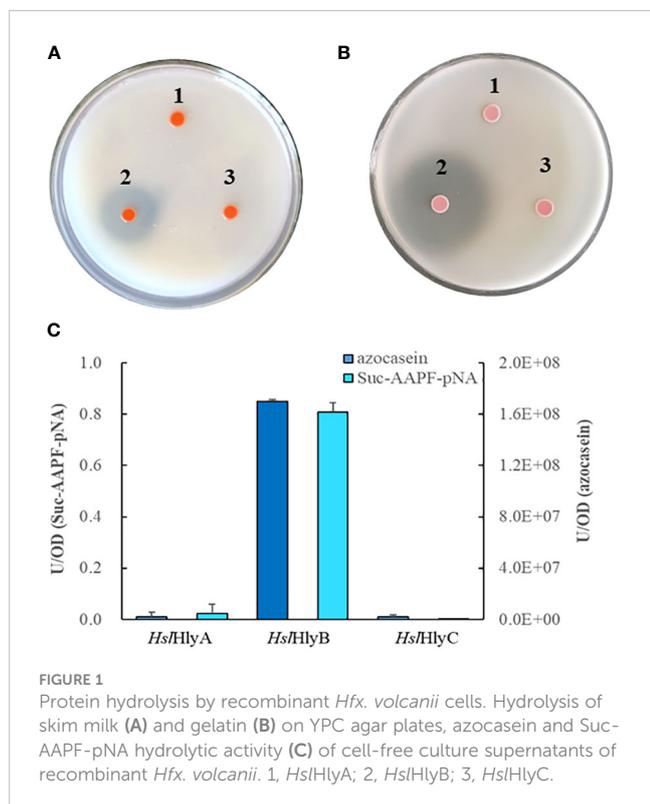
Effect of CTEs on *Hsl*HlyB activity

CTE is prevalent in halolysins. It has important effects on enzyme activity and enzyme secretion. The novel C-terminal domains of *Hsl*HlyB consist of a PKD domain and a PPC domain. To investigate the effect of CTEs on enzymatic activity, *Hsl*HlyBΔPKD and *Hsl*HlyBΔCTE were constructed, with deletion of *Hsl*HlyB PKD domain and the whole CTE domain. In contrast to the strain expressing wild-type *Hsl*HlyB, the recombinant strains showed reductions in hydrolysis circle size on milk plates and also decreased activities against azocasein and Suc-AAPF-pNA (Figures 2B, C). The extracellular supernatant activity of the recombinant strain with *Hsl*HlyBΔPKD towards azocasein and Suc-AAPF-pNA decreased by 54.5% and 56.5%, respectively. The extracellular supernatant activity of the strain expressing *Hsl*HlyBΔCTE showed undetectable protease activity.

The CTE domain is self-stabilizing and can fold independently. Our previous study found that CTE domain can be functionally interchangeable among halolysins (Hou et al., 2020). To investigate the effect of CTE on *Hsl*HlyB activity, three chimeras, *Hsl*HlyB-HlyAC, *Hsl*HlyB-R4C and *Hsl*HlyB-NepC, namely, *Hsl*HlyB catalytic domain with the CTE of HlyA from *Hcc. salifodinae* (119 aa), R4 from *Hfx. mediterranei* (114 aa) and Nep from *Nab. magadii* (131 aa) (Kamekura et al., 1996; De Castro et al., 2008; Hou et al., 2020) (Figure 2A) were heterologously expressed in *Hfx. volcanii* H1424. The extracellular proteolytic activities were determined. The strains expressing *Hsl*HlyB-NepC cannot hydrolyze milk and had no activity towards azocasein and Suc-AAPF-pNA (Figures 2B, C). The strains expressing *Hsl*HlyB-HlyAC can hydrolyze milk. The hydrolysis zone of *Hsl*HlyB-R4C expressing strains is larger than those of *Hsl*HlyB-HlyAC expressing strains, while both are smaller than that of wildtype *Hsl*HlyB expressing strains (Figure 2B). The activity of the culture supernatant of cells expressing *Hsl*HlyB-HlyAC towards azocasein and Suc-AAPF-pNA decreased by 89.5% and 87.9%, respectively, and that of *Hsl*HlyB-R4C decreased by 93.9% and 89.6%, respectively (Figure 2C). The extracellular activities of recombinant strains expressing *Hsl*HlyB-HlyAC and *Hsl*HlyB-R4C towards tetrapeptide, a small molecule substrate, decreased less than that of azocasein, indicating that the CTE may affect the hydrolysis ability towards different substrates. The CTE of halolysins R4 from *Hfx. mediterranei*, HlyA from *Hcc. salifodinae*, Nep from *Nab. magadii* significantly reduced or abolished the extracellular enzyme activity of *Hsl*HlyB after substitution. The decreased extracellular enzyme activity is possibly because heterologous CTEs affect the correct folding of the *Hsl*HlyB catalytic domain. The effect of CTEs on halolysin activity remains to be investigated in depth.

Purification and refolding of *Hsl*HlyB and *Hsl*HlyBΔCTE

*Hsl*HlyB and *Hsl*HlyBΔCTE with 6×His tag at the C-terminus were expressed in *E. coli* BL21 (DE3). Both intracellular lysate and culture supernatant of *E. coli* were without protease activity after induced expression. The protease precursors were obtained by affinity chromatography and confirmed by MALDI-TOF/TOF MS
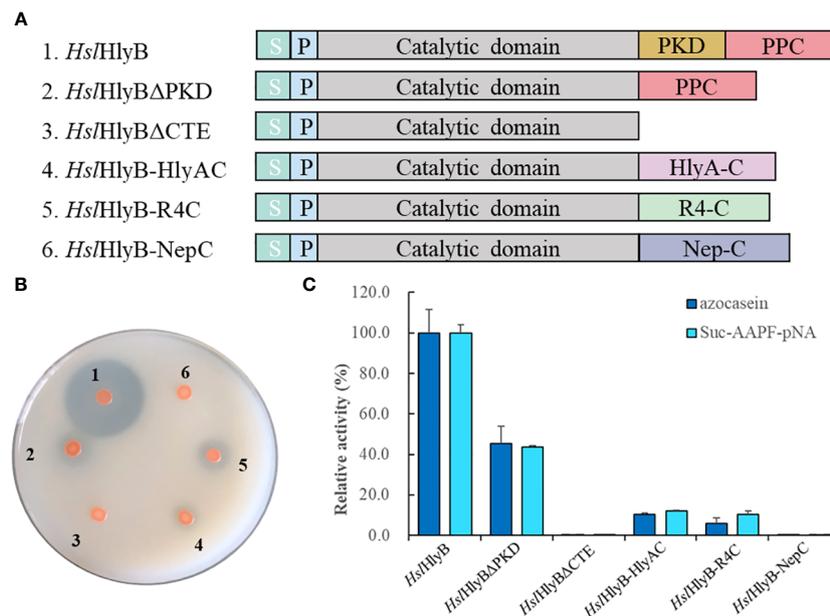
FIGURE 2
Effect of CTE on *Hsl*HlyB activity. **(A)** Domain arrangement of *Hsl*HlyB and the chimeras. S: signal peptide, P: propeptide, PKD: polycystic kidney disease domain, PPC: prepeptidase C-terminal domain, HlyA-C:C-terminal extension of HlyA, R4-C: C-terminal extension of R4, Nep-C: C-terminal extension of Nep. **(B)** Hydrolysis of skim milk by recombinant *Hfx. volcanii* cells on YPC agar plates. **(C)** Azocasein and Suc-AAPF-pNA hydrolytic activity of cell-free culture supernatants of recombinant *Hfx. volcanii*. 1, *Hsl*HlyB; 2, *Hsl*HlyBΔPKD; 3, *Hsl*HlyBΔCTE; 4, *Hsl*HlyB–HlyAC; 5, *Hsl*HlyB-R4C; 6, *Hsl*HlyB–NepC.

(Figure 3). The molecular mass of the protease precursor estimated from the *Hsl*HlyB protein sequence was 63 kDa, while the apparent molecular masses from SDS-PAGE were 108 kDa and 96 kDa. The presence of two bands of *Hsl*HlyB precursor was due to the excision of N-terminal sequences (Figure 3C). As for *Hsl*HlyBΔCTE, a single band with an apparent molecular mass of about 68 kDa was obtained. The phenomenon that the apparent molecular mass is much larger than the predicted molecular mass is common in the SDS-PAGE analysis of halophilic proteins (Alves et al., 2004; Karan et al., 2013; Gao et al., 2017), which is caused by the decrease of protein migration rate with the high content of acidic amino acids in halophilic proteins.

On-column refolding was performed to allow the mature enzymes to be obtained by self-processing with its C-terminus bound to Ni-agarose. The refolding product of *Hsl*HlyB revealed two bands on SDS-PAGE gel, and that of *Hsl*HlyBΔCTE revealed a major band (Figures 3A, B). The *Hsl*HlyB refolding product consisted of mature enzyme, and also CTE fraction from autodegradation (Figure 3C). The refolding product of *Hsl*HlyBΔCTE corresponded to the catalytic domain identified by MALDI-TOF/TOF MS (Figure 3C). The refolding products were further purified by Superdex 200 GL column (Figures S2A, B). The purified products each revealed a major band on SDS-PAGE gel (Figures S2C, D). Combined with the molecular sieve profiles of protein standards with known molecular mass, the molecular mass of *Hsl*HlyB and *Hsl*HlyBΔCTE were estimated to be 42 kDa and 20 kDa, respectively. Halolysins, like most subtilases, are autocatalyzed into mature enzymes by *cis*- and *trans*-processing (Ruiz et al., 2012; Du et al., 2015). The purified precursors could autocatalyze to

mature enzymes in high salt environments. Both CTE truncates and wild-type proteases were able to mature *in vitro*. However, when *Hsl*HlyBΔCTE was expressed in *Hfx. volcanii*, the recombinant strains showed no extracellular protease activity, similarly to the removal of the CTE from halolysin R4 and SptA (Kamekura et al., 1996; Xu et al., 2011). The immunoblot analysis of CTE truncates of SptA showed that no pro- or mature forms were secreted into the extracellular matrix (Xu et al., 2011). In contrast, the studies on Nep from *Nab. magadii* revealed that the absence of CTE did not affect the secretion and maturation of the enzyme in the halophilic archaeon (Marem et al., 2018). These results indicated that CTEs may have different effects on the structure of other domains *in vivo*, thus affecting maturation or secretion for different halolysins. In the case of *Hsl*HlyB in this study, as a subtilisin family enzyme with two β-sandwich domains at the C-terminus, its domain distribution is identical to that of fervidolysin (from *Fervidobacterium pennivorans*) with a sequence identity of 37.69%. The crystal structure of fervidolysin (PDB accession no. 1R6V) suggests that its CTE can create an open hydrophobic pocket that contributes to the fixation of the N-terminal elongated chain of the N-terminal pre-peptide domain (Kim et al., 2004). The study of the metalloprotease PrtV (from *Vibrio cholerae*) showed that the PKD domain with calcium ions controls the flexibility of the protein domain linker (Edwin et al., 2013). The CTE of *Hsl*HlyB probably affects the domain linker of the pre-peptide and plays a regulatory role in proper folding, thus affecting the secretion and autocatalytic maturation of the enzyme *in vivo*. CTE has also been reported to be involved in maintaining the stability of the catalytic domain. The halolysin SptA from *Natrinema* sp. J7 without CTE
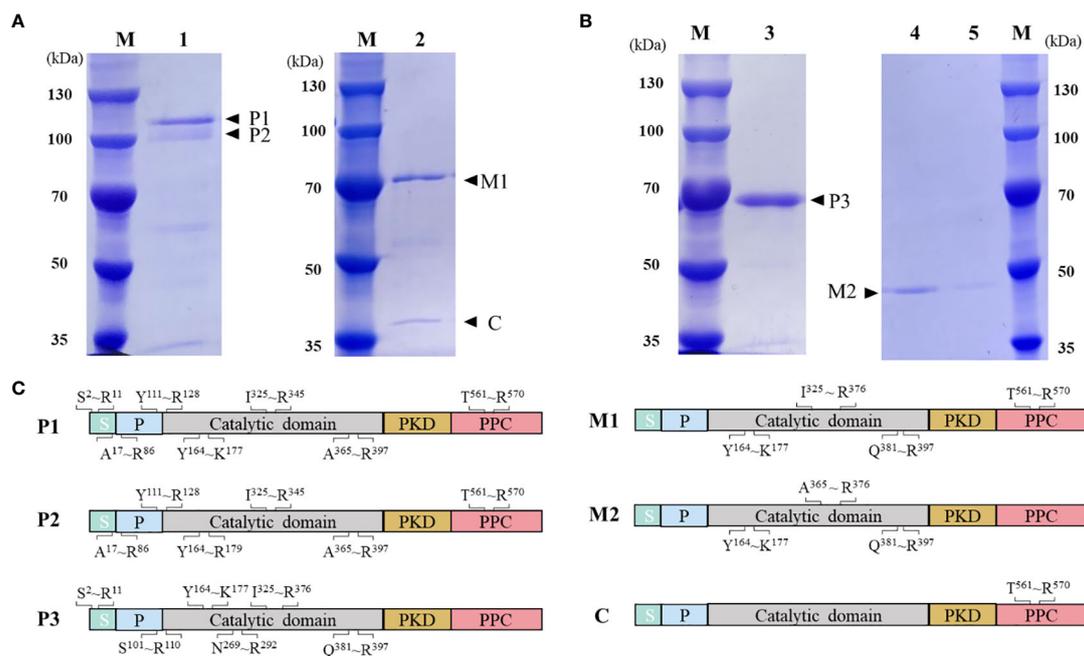
FIGURE 3

Purification and on-column refolding of *Hsl*HlyB and *Hsl*HlyBΔCTE. **(A)** SDS-PAGE analysis of *Hsl*HlyB precursor and mature *Hsl*HlyB. **(B)** SDS-PAGE analysis of *Hsl*HlyBΔCTE precursor and mature *Hsl*HlyBΔCTE. **(C)** MALDI-TOF/TOF MS analysis of protein bands in SDS-PAGE analysis. Sequenced tryptic peptides are marked. P1 and P2: *Hsl*HlyB precursor, P3, *Hsl*HlyBΔCTE precursor; C, the cleaved C-terminal fragments; M1, mature *Hsl*HlyB; M2, mature *Hsl*HlyBΔCTE; M, marker; lane 1, recombinant *Hsl*HlyB precursor purified under denaturing conditions; lane 2, refolded product of *Hsl*HlyB precursor; lane 3, recombinant *Hsl*HlyBΔCTE precursor purified under denaturing conditions; lane 4-5, refolded product of *Hsl*HlyBΔCTE precursor; S, signal peptide; P, propeptide; PKD, polycystic kidney disease domain; PPC, prepeptidase C-terminal domain.

would be more prone to enzyme autolysis (Xu et al., 2011). However, the catalytic domain of *Hsl*HlyB remained stable *in vitro* in the absence of the entire CTE. The structure of halolysins would help dissect the underlying mechanisms.

Effect of temperature, pH and NaCl concentration on *Hsl*HlyB and *Hsl*HlyBΔCTE activity

The optimum reaction temperature for *Hsl*HlyB and *Hsl*HlyBΔCTE was 50°C. They were able to maintain more than 79% and 88% of the maximum enzyme activity at 40-60°C, respectively (Figures 4A, B). The thermal stability of the enzymes was studied based on the residual enzyme activities of the proteases after incubation at different temperatures (Figures 4C, D). The activity of *Hsl*HlyB decreased with increasing incubation time at 60°C, but it could still maintain about 80% of the original enzyme activity after incubation for 60 min. *Hsl*HlyB maintained about 91% of the original enzyme activity after incubation at 50°C for 60 min, and the activity of *Hsl*HlyB did not change significantly after incubation at 30-40°C. Notably, the activity of *Hsl*HlyBΔCTE remained essentially the same after incubation at 30-60°C for 0-60 min. The residual activity of Nep from *Nab. magadii* was >30% of original activity after incubation at 60°C for 2 h (Giménez et al., 2000), that of Hly$_{Hap}$ from *Haladaptatus* sp. DYF46 was 33.9% after incubation at 60°C for 1 h (Hou et al., 2022), and that of Hly from *Hgn. rubrum* RO2-11 was <20% after incubation

at 60°C for 1 h (Gao et al., 2017). Both *Hsl*HlyB and *Hsl*HlyBΔCTE have good thermal stability, and *Hsl*HlyBΔCTE shows better thermal stability than wild type enzyme.

The activities of *Hsl*HlyB and *Hsl*HlyBΔCTE in Tris-HCl buffer (pH 7.5-9.0) showed different trends, with *Hsl*HlyB activity increasing and then decreasing, and *Hsl*HlyBΔCTE activity decreasing within pH rise. Their optimal pH was 8.5 and 7.5, respectively (Figures 5A, B). *Hsl*HlyB displayed >83% of the maximal activity within pH 7.5-9.0, and *Hsl*HlyBΔCTE displayed >74% of the maximal activity within pH 7.5-8.5. The activities of *Hsl*HlyB and *Hsl*HlyBΔCTE did not significantly change from 0-60 min when the proteases were incubated at different pH (Figures 5C, D), indicating their good pH stability.

The activities of *Hsl*HlyB and *Hsl*HlyBΔCTE increased with increasing NaCl concentrations at NaCl < 3 M. They maintained more than 93% of the highest catalytic activity in 3-4 M NaCl. Their optimum NaCl concentrations were 3.5 M and 3 M (Figures 6A, B). The salinity stability of *Hsl*HlyB and *Hsl*HlyBΔCTE was similar (Figures 6C, D). The enzyme activity decreased slightly (<10%) after 60 min incubation at NaCl concentrations of 2-4 M. The activity decreased rapidly after 0-60 min of incubation with a NaCl concentration of 0.8 M. The inactivation rate of *Hsl*HlyBΔCTE was faster than that of *Hsl*HlyB. *Hsl*HlyB and *Hsl*HlyBΔCTE were stable at NaCl concentrations >2 M and inactivated at low salt environments. Most halolysin activities increase and then decrease with increasing salt concentration, and the optimal salt concentration for the catalytic reaction is around 2-3 M
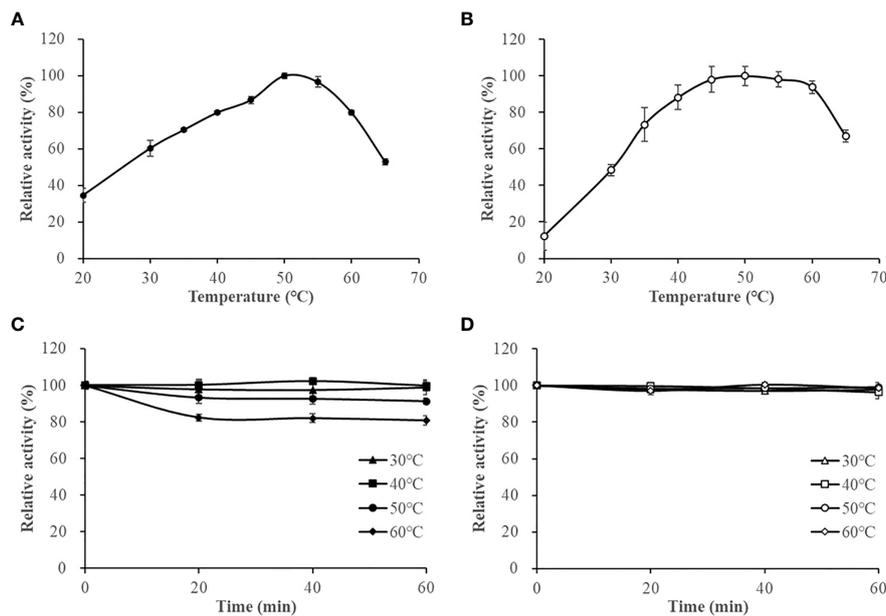
FIGURE 4
The effect of temperature on *Hsl*HlyB **(A)** and *Hsl*HlyBΔCTE activity **(B)**, and the thermal stability of *Hsl*HlyB **(C)** and *Hsl*HlyBΔCTE **(D)**. In **(A, B)**, relative activities were calculated with the maximal activity defined as 100%. In **(C, D)**, the initial enzyme activity was set as 100%, upon which the relative activities of enzymes after incubation at different temperatures for 20, 40 or 60 min were calculated. Mean ± SD of three biological replicates.

(Kamekura et al., 1996; Giménez et al., 2000; Shi et al., 2006; Vidyasagar et al., 2006; Elbanna et al., 2015; Dammak et al., 2016; Hou et al., 2021). In this study, the catalytic activities of *Hsl*HlyB and *Hsl*HlyBΔCTE increased and then remained stable with increasing salt concentration. They reached the highest activity at >3 M salt concentration, thus were more suitable for catalysis in high salt environment.

Effect of metal ions, solvents, surfactants and inhibitors on *Hsl*HlyB and *Hsl*HlyBΔCTE activity

Metal ions are often used as enzyme cofactors. Different metal ions were reported to have different effects on halolysin activity. For *Hsl*HlyB, Fe^{3+}, K^+, Mg^{2+} and Mn^{2+} had almost no effect on the
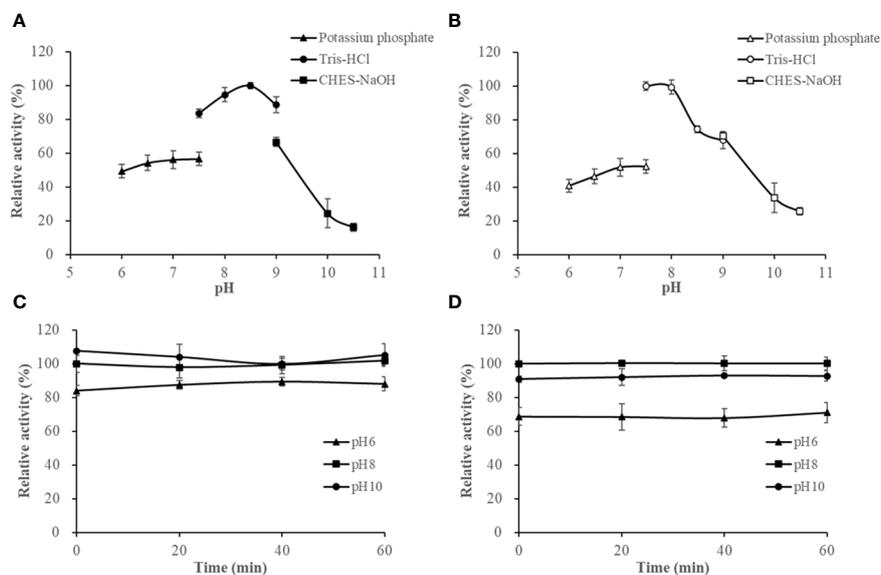

FIGURE 5
The effect of pH on *Hsl*HlyB **(A)** and *Hsl*HlyBΔCTE activity **(B)**, and the pH stability of *Hsl*HlyB **(C)** and *Hsl*HlyBΔCTE **(D)**. In **(A, B)**, relative activities were calculated with the maximal activity defined as 100%. In **(C, D)**, the initial enzyme activity at pH 8.0 was set as 100%, upon which the relative activities of enzymes after incubation at different pH for 20, 40 or 60 min were calculated. Mean ± SD of three biological replicates.
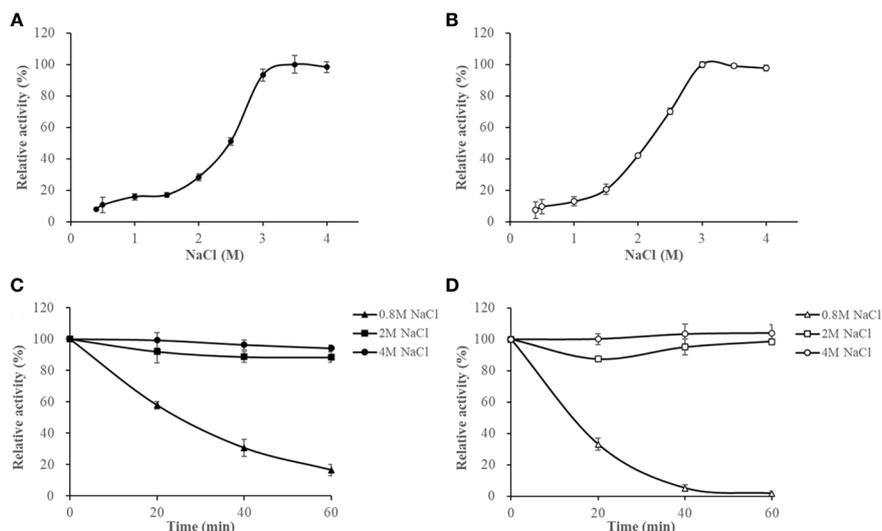
FIGURE 6
The effect of NaCl on HslHlyB **(A)** and HslHlyBΔCTE activity **(B)**, and the salinity stability of HslHlyB **(C)** and HslHlyBΔCTE **(D)**. In **(A, B)**, relative activities were calculated with the maximal activity defined as 100%. In **(C, D)**, the initial enzyme activity was set as 100%, upon which the relative activities of enzymes after incubation at different salinities for 20, 40 or 60 min were calculated. Mean ± SD of three biological replicates.

enzyme activity, Ca^{2+} and Sr^{2+} slightly promoted the enzyme activity, and Cu^{2+} and Zn^{2+} inhibited 55.1% and 29.6% of the enzyme activity (Figure 7A). For HslHlyBΔCTE, K^+, Ca^{2+}, Mg^{2+}, Sr^{2+} slightly promoted the enzyme activity, Fe^{3+}, Cu^{2+}, Mn^{2+} and Zn^{2+} inhibited 25.2%, 44.4%, 56.5% and 22.4% of the enzyme activity (Figure 7A). Cu^{2+} and Zn^{2+} significantly inhibited both HslHlyB and HslHlyBΔCTE activities. Fe^{3+} and Mn^{2+} had a much higher inhibitory effect on the activity of HslHlyBΔCTE than HslHlyB. The CTE domain of HslHlyB affects the tolerance of halolysin to some metal ions.

Different solvents and surfactants decreased the activity of HslHlyB and HslHlyBΔCTE to different degrees (Table 1; Figure 7B). The solvents in which the HslHlyB activity remained above 80% were glycerol, dimethyl sulfoxide (DMSO), and polyethylene glycol (PEG) 600. Isopropyl alcohol and SDS had a significant inhibitory effect on HslHlyB activity (<50%). The solvents in which HslHlyBΔCTE activity maintained more than 80% were methanol, glycerol, acetone, DMSO, dimethylformamide (DMF), Tween 20, Tween 80 and PEG 600. Isopropanol, SDS and TritonX-100 had a significant inhibitory effect on HslHlyBΔCTE activity (<50%). HslHlyBΔCTE had a better tolerance to organic solvents than wild type enzyme.

The effect of protease inhibitors on HslHlyB and HslHlyBΔCTE activity was essentially the same (Figure 7B). 4 mM PMSF completely inhibited the activity of both enzymes, EDTA reduced their activity by 93.0% and 94.3% respectively, Pepstatin A reduced their activity by 4.3%, DTT reduced their activity by 60.3% and 59.1% respectively, and PCMB increased their enzymatic activity by 14.1% and 9.2%. This suggested that HslHlyB and HslHlyBΔCTE may be metal ion-dependent serine proteases and that disulfide bonds are important for their activity.

Determination of K_m, V_{max} and proteolytic activity

The data obtained were well described by the Michaelis-Menten equation using azocasein and Suc-AAPF-pNA as reaction substrates (Figure 8). The K_m and V_{max} of HslHlyB and HslHlyBΔCTE were 0.07 mM, 2814 U/min/mg and 0.16 mM, 4485 U/min/mg against azocasein, 0.36 mM, $8.4×10^9$ μmol/min/mg and 0.27 mM, $2.1×10^{10}$ μmol/min/mg against Suc-AAPF-pNA. HslHlyBΔCTE showed higher maximum reaction rates for both substrates, 1.6-fold and 2.5-fold of the wild type, respectively. HslHlyBΔCTE had a higher K_m value for azocasein and a lower K_m value for Suc-AAPF-pNA than wild type. The above results indicated that HslHlyBΔCTE had better catalytic effect on small molecule substrates, as shown by higher maximum reaction rate and higher substrate affinity. As for azocasein, HslHlyBΔCTE had higher maximum reaction rate but lower substrate affinity than wild-type. Similar phenomenon on the hydrolysis of small peptide substrates by HslHlyB and HslHlyBΔCTE has been reported for Nep from $Nab.$ $magadii$ (De Castro et al., 2008). CTE are involved in protein-protein interactions. PKD domain does not show any proteolysis activity, but can adsorb and swell insoluble proteins (Chen et al., 2007). The PPC domain also plays a key role in binding to the substrate (Xu et al., 2011; He et al., 2012). In the present study, CTE of HslHlyB also affected the affinity of the enzyme against the protein substrate.

HslHlyB and HslHlyBΔCTE can hydrolyze casein, bovine hemoglobin, azocasein, skim milk, gelatin, egg albumin and bovine serum albumin, with the highest catalytic activity towards casein (Figure 7C). Their wide substrate spectra make them good candidates for industrial applications.
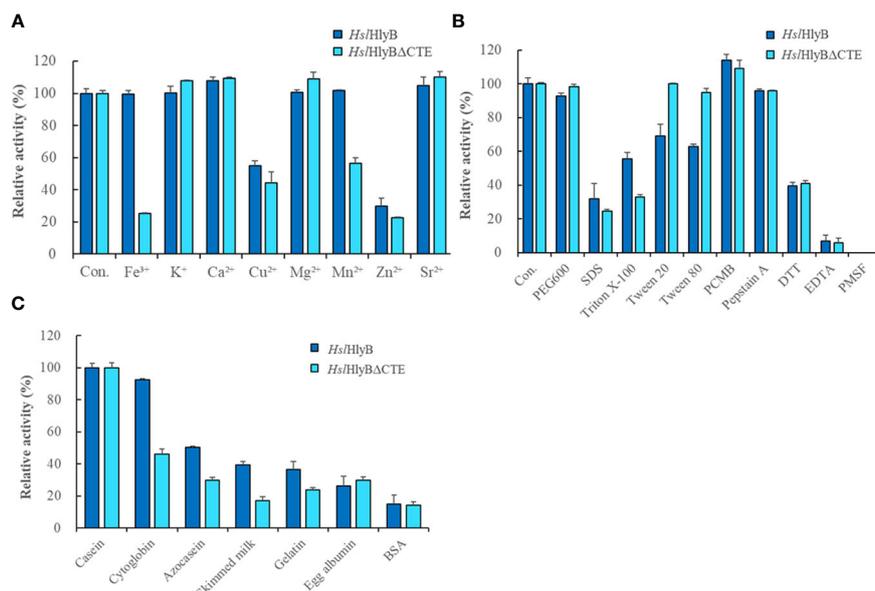
FIGURE 7
The effect of metal ions **(A)**, detergents, and inhibitors **(B)** on *Hsl*HlyB and *Hsl*HlyBΔCTE activity, and proteolytic activity against different substrates of *Hsl*HlyB and *Hsl*HlyBΔCTE **(C)**. Con.: control. In **(A, B)**, the enzyme assay was carried out with different metal ions at the concentration of 5 mM, with 10% detergents, 1 mM PCMB, 10 mM Pepstatin A, 10 mM DTT, 5 mM EDTA, 4 mM PMSF. In **(C)**, the protein substrate concentration of 5 g/L was used and the enzyme activity was measured by the amount of tyrosine produced. Mean ± SD of three biological replicates.

Hydrolysis of soybean protein isolate by *Hsl*HlyB and *Hsl*HlyBΔCTE

High-salt fermentation of soybeans is a common production process for soy sauce. The hydrolysis of soybean protein contributes the flavor and raw material utilization of soy sauce. To expand the application of halolysin in high-salt foods, the peptides from hydrolyzed soybean isolate protein by *Hsl*HlyB and *Hsl*HlyBΔCTE were identified. 128 peptides with an average molecular mass of 1928.87 Da and an average peptide chain length of 16.2 amino acids were identified from soybean protein isolate hydrolysate by *Hsl*HlyB (Table S3). 205 peptides with an average molecular mass of 1894.01 Da and an average peptide chain length of 15.6 amino

acids were identified from soybean protein isolate hydrolysate by *Hsl*HlyBΔCTE (Table S3). The average molecular mass of the peptide profile after hydrolysis by *Hsl*HlyBΔCTE was smaller, and the average length of the peptide chains was shorter. Soybean protein isolate hydrolysates by both enzymes showed the highest peptide content in the range of 11-20 amino acids. The amino acid number distribution of peptides generated by *Hsl*HlyB was more uniform. The cleavage sites of *Hsl*HlyB and *Hsl*HlyBΔCTE were counted based on the peptides identified from the soybean protein isolate hydrolysates (Tables S4, 5). Similar to most serine proteases, *Hsl*HlyB and *Hsl*HlyBΔCTE do not have specific cleavage sites, but they seem to prefer to cleave proteins with acidic amino acids at the P1' position and proline at the P2 position. Halolysins exert endo-

TABLE 1 Effect of solvents on *Hsl*HlyB and *Hsl*HlyBΔCTE activity.

Solvents	log $P_{o/w}$ [a]	*Hsl*HlyB Relative activity (%) [b]	*Hsl*HlyBΔCTE Relative activity (%) [b]
Glycerol	-1.76	94.8 ± 5.3	94.2 ± 2.9
DMSO	-1.35	81.0 ± 2.3	98.2 ± 0.7
DMF	-1.0	70.6 ± 1.5	81.2 ± 0.3
Methanol	-0.82	75.0 ± 5.0	83.3 ± 0.9
Acetonitrile	-0.34	69.6 ± 2.2	75.9 ± 1.3
Ethanol	-0.31	56.8 ± 1.0	50.5 ± 0.7
Acetone	-0.24	72.1 ± 1.1	87.4 ± 1.7
Isopropanol	0.05	41.6 ± 3.2	40.8 ± 0.9

[a]log $P_{o/w}$ represents a quantitative measure of solvent polarity.
[b]The activity assayed in the absence of organic solvents was defined as the control activity of 100%. The organic solvent is added to the reaction system at 5% (v/v). Mean ± SD of three biological replicates.
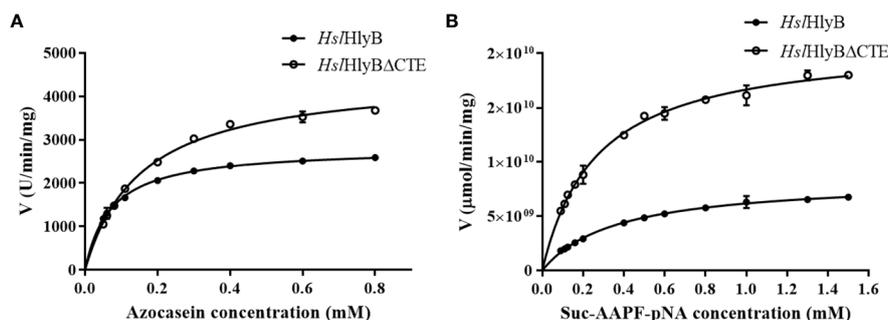
FIGURE 8

Michaelis-Menten graph of *Hsl*HlyB and *Hsl*HlyBΔCTE against azocasein **(A)** and Suc-AAPF-pNA **(B)**. Mean ± SD of three biological replicates.

protease activity that hydrolyze protein into peptides. *Hsl*HlyB and *Hsl*HlyBΔCTE can hydrolyze a wide range of protein substrates, such as soybean protein, which is mainly hydrolyzed to peptides of 11-20 amino acids. The variety of soybean protein hydrolysates were important compounds for soy sauce flavor. There are also several reports on halolysins for accelerating fish sauce fermentation in high-salt or low-salt conditions (Akolkar et al., 2010; Gao et al., 2017; Hou et al., 2020). Halolysins thus revealed potential application in food industry.

Conclusion

In summary, the gene *hslhlyB* encodes a novel halolysin with PKD and PPC domains at the C-terminus in *Hsl. pelagica* DL-M4[T]. *Hsl*HlyB and *Hsl*HlyBΔCTE, like most halolysins, were highly salt tolerant. They show relatively good tolerance to organic solvents and good thermal stability. The absence of CTE of *Hsl*HlyB resulted in the increased activity and thermal stability of the protease while maintaining similar catalytic properties. The CTE affected maturation or secretion of *Hsl*HlyB *in vivo*, while it had no effect on maturation *in vitro*. Based on the biochemical characterization of halolysin from *Hsl. pelagica* DL-M4[T], *Hsl*HlyB and in particular the CTE deletion mutant, are promising salt-tolerant protease candidates for high-salt food processing applications, such as protein hydrolysis in soy sauce.

Data availability statement

The datasets presented in this study can be found in online repositories. The names of the repository/repositories and accession number(s) can be found in the article/Supplementary Material.

Author contributions

DH: conducted experiments, analyzed data and wrote the manuscript, acquired funding. JH: conceived and designed research, wrote and reviewed the manuscript. H-LC: supervised experiments, reviewed and edited the manuscript, acquired funding. All authors contributed to the article and approved the submitted version.

Funding

Conflict of interest

The authors declare that the research was conducted in the absence of any commercial or financial relationships that could be construed as a potential conflict of interest.

Publisher's note

All claims expressed in this article are solely those of the authors and do not necessarily represent those of their affiliated organizations, or those of the publisher, the editors and the reviewers. Any product that may be evaluated in this article, or claim that may be made by its manufacturer, is not guaranteed or endorsed by the publisher.

Supplementary material

The Supplementary Material for this article can be found online at: https://www.frontiersin.org/articles/10.3389/fmars.2023.1166287/full#supplementary-material

References

Akolkar, A. V., Deshpande, G. M., Raval, K. N., Durai, D., Nerurkar, A. S., and Desai, A. J. (2008). Organic solvent tolerance of *Halobacterium* sp. SP1 (1) and its extracellular protease. *J. Basic Microb.* 48, 421–425. doi: 10.1002/jobm.200800012

Akolkar, A. V., Durai, D., and Desai, A. J. (2010). *Halobacterium* sp. SP1 (1) as a starter culture for accelerating fish sauce fermentation. *J. Appl. Microbiol.* 109, 44–53. doi: 10.1111/j.1365-2672.2009.04626.x

Altschul, S. F., Madden, T. L., Schäffer, A. A., Zhang, J., Zhang, Z., Miller, W., et al. (1997). Gapped BLAST and PSI-BLAST: a new generation of protein database search programs. *Nucleic Acids Res.* 25, 3389–3402. doi: 10.1093/nar/25.17.3389

Alves, V. S., Pimenta, D. C., Sattlegger, E., and Castilho, B. A. (2004). Biophysical and functional characterization of Gir2, a highly acidic protein of *Saccharomyces cerevisiae*. *Biochem. Biophys. Res. Commun.* 314, 229–234. doi: 10.1016/j.bbrc.2003.12.086

Amoozegar, M. A., Siroosi, M., Atashgahi, S., Smidt, H., and Ventosa, A. (2017). Systematics of haloarchaea and biotechnological potential of their hydrolytic enzymes. *Microbiology* 163, 623–645. doi: 10.1099/mic.0.000463

Armenteros, J. J. A., Tsirigos, K. D., Sønderby, C. K., Petersen, T. N., Winther, O., Brunak, S., et al. (2019). SignalP 5.0 improves signal peptide predictions using deep neural networks. *Nat. Biotechnol.* 37, 420. doi: 10.1038/s41587-019-0036-z

Bradford, M. M. (1976). A rapid and sensitive method for the quantitation of microgram quantities of protein utilizing the principle of protein-dye binding. *Anal. Boichem.* 72, 248–254. doi: 10.1016/0003-2697(76)90527-3

Chaveesuk, R., Smith, J. P., and Simpson, B. K. (1994). Production of fish sauce and acceleration of sauce fermentation using proteolytic enzymes. *J. Aquat. Food. Prod. T.* 2, 59–77. doi: 10.1300/J030v02n03_05

Chen, S. X., Sun, S. Q., Wang, R., Feng, H. L., and Xiang, H. (2021). *Haloferax mediterranei* halolysin R4 confers antagonistic and defensive capabilities. *Appl. Environ. Microb.* 87, e02889–e02820. doi: 10.1128/AEM.02889-20

Chen, X. L., Xie, B. B., Lu, J. T., He, H. L., and Zhang, Y. (2007). A novel type of subtilase from the psychrotolerant bacterium *Pseudoalteromonas* sp. SM9913: catalytic and structural properties of deseasin MCP-01. *Microbiology* 153, 2116–2125. doi: 10.1099/mic.0.2007/006056-0

Cui, H. L., and Dyall Smith, M. L. (2021). Cultivation of halophilic archaea (class *Halobacteria*) from thalassohaline and athalassohaline environments. *Mar. Life. Sci. Tech.* 3, 243–251. doi: 10.1007/s42995-020-00087-3

Cui, H. L., Yang, X., and Mou, Y. Z. (2011). *Salinarchaeum laminariae* gen. nov., sp. nov.: a new member of the family *Halobacteriaceae* isolated from salted brown alga *Laminaria*. *Extremophiles* 15, 625–631. doi: 10.1007/s00792-011-0393-0

Dammak, D. F., Smaoui, S. M., Ghanmi, F., Boujelben, I., and Maalej, S. (2016). Characterization of halo-alkaline and thermostable protease from *Halorubrum ezzemoulense* strain ETR14 isolated from sfax solar saltern in Tunisia. *J. Basic Microb.* 56, 337–346. doi: 10.1002/jobm.201500475

De Castro, R. E., Ruiz, D. M., Giménez, M. I., Silveyra, M. X., Paggi, R. A., and Maupin-Furlow, J. A. (2008). Gene cloning and heterologous synthesis of a haloalkaliphilic extracellular protease of *Natrialba magadii* (Nep). *Extremophiles* 12, 677. doi: 10.1007/s00792-008-0174-6

Du, X., Li, M. R., Tang, W., Zhang, Y. X., Zhang, L., Wang, J., et al. (2015). Secretion of tat-dependent halolysin SptA capable of autocatalytic activation and its relation to haloarchaeal growth. *Mol. Microbiol.* 96, 548–565. doi: 10.1111/mmi.12955

Edwin, A., Rompikuntal, P., Bjorn, E., Stier, G., Wai, S. N., and Sauer-Eriksson, A. E. (2013). Calcium binding by the PKD1 domain regulates interdomain flexibility in *Vibrio cholerae* metalloprotease PrtV. *FEBS Open Bio.* 3, 263–270. doi: 10.1016/j.fob.2013.06.003

Elbanna, K., Ibrahim, I. M., and Revol Junelles, A. M. (2015). Purification and characterization of halo-alkali-thermophilic protease from *Halobacterium* sp. strain HP25 isolated from raw salt, lake qarun, fayoum, Egypt. *Extremophiles* 19, 763–774. doi: 10.1007/s00792-015-0752-3

Elsztein, C., Herrera Seitz, M. K., Sanchez, J. J., and De Castro, R. E. (2001). Autoproteolytic activation of the haloalkaliphilic archaeon *Natronococcus occultus* extracellular serine protease. *J. Basic Microb.* 41, 319–327. doi: 10.1002/1521-4028(200112)41:6<319::AID-JOBM319>3.0.CO;2-8

Finn, R. D., Clements, J., and Eddy, S. R. (2011). HMMER web server: interactive sequence similarity searching. *Nucleic Acids Res.* 39, W29–W37. doi: 10.1093/nar/gkr367

Gao, R. C., Shi, T., Liu, X. D., Zhao, M. Q., Cui, H. L., and Yuan, L. (2017). Purification and characterisation of a salt-stable protease from the halophilic archaeon *Halogranum rubrum*. *J. Sci. Food Agr.* 97, 1412–1419. doi: 10.1002/jsfa.7879

Gao, X., Wang, J., Yu, D. Q., Bian, F., Xie, B. B., Chen, X. L., et al. (2010). Structural basis for the autoprocessing of zinc metalloproteases in the thermolysin family. *Proc. Natl. Acad. Sci. U.S.A.* 107, 17569–17574. doi: 10.1073/pnas.1005681107

Giménez, M. I., Studdert, C. A., Sánchez, J. J., and De Castro, R. E. (2000). Extracellular protease of *Natrialba magadii*: purification and biochemical characterization. *Extremophiles* 4, 181–188. doi: 10.1007/s007920070033

Han, D., and Cui, H. L. (2020). *Halostella pelagica* sp. nov. and *Halostella litorea* sp. nov., isolated from salted brown alga *Laminaria*. *Int. J. Syst. Evol. Micr.* 70, 1969–1976. doi: 10.1099/ijsem.0.004003

He, H. L., Guo, J., Chen, X. L., Xie, B. B., Zhang, X. Y., Yu, Y., et al. (2012). Structural and functional characterization of mature forms of metalloprotease E495 from arctic sea-ice bacterium *Pseudoalteromonas* sp. SM495. *PloS One* 7, e35442. doi: 10.1371/journal.pone.0035442

Hou, J., Han, D., Zhou, Y., Li, Y., and Cui, H. L. (2020). Identification and characterization of the gene encoding an extracellular protease from haloarchaeon *Halococcus salifodinae*. *Microbiol. Res.* 236, 126468. doi: 10.1016/j.micres.2020.126468

Hou, J., Li, S. Y., Zhao, Y. J., and Cui, H. L. (2022). A novel halolysin without c-terminal extension from an extremely halophilic archaeon. *Appl. Microbiol. Biot.* 106, 3009–3019. doi: 10.1007/s00253-022-11903-4

Hou, J., Yin, X. M., Li, Y., Han, D., Lü, B., Zhang, J. Y., et al. (2021). Biochemical characterization of a low salt-adapted extracellular protease from the extremely halophilic archaeon *Halococcus salifodinae*. *Int. J. Biol. Macromol.* 176, 253–259. doi: 10.1016/j.ijbiomac.2021.02.081

Huang, J. F., Wu, R. B., Liu, D., Liao, B. Q., Lei, M., Wang, M., et al. (2019). Mechanistic insight into the binding and swelling functions of prepeptidase c-terminal (PPC) domains from various bacterial proteases. *Appl. Environ. Microb.* 85, e00611–e00619. doi: 10.1128/AEM.00611-19

Huang, J., Wu, C., Liu, D., Yang, X., Wu, R., Zhang, J., et al. (2017). C-terminal domains of bacterial proteases: structure, function and the biotechnological applications. *J. Appl. Microbiol.* 122, 12–22. doi: 10.1111/jam.13317

Jaouadi, B., Ellouz-Chaabouni, S., Rhimi, M., and Bejar, S. (2008). Biochemical and molecular characterization of a detergent-stable serine alkaline protease from *Bacillus pumilus* CBS with high catalytic efficiency. *Biochimie* 90, 1291–1305. doi: 10.1016/j.biochi.2008.03.004

Jumper, J., Evans, R., Pritzel, A., Green, T., Figurnov, M., Ronneberger, O., et al. (2021). Highly accurate protein structure prediction with AlphaFold. *Nature* 596, 583–589. doi: 10.1038/s41586-021-03819-2

Kamekura, M., Seno, Y., and Dyall Smith, M. (1996). Halolysin R4, a serine proteinase from the halophilic archaeon *Haloferax mediterranei*: gene cloning, expression and structural studies. *Biochim. Biophys. Acta-Protein Struct. Mol. Enzymol.* 1294, 159–167. doi: 10.1016/0167-4838(96)00016-7

Kamekura, M., Seno, Y., Holmes, M. L., and Smith, M. L. D. (1992). Molecular cloning and sequencing of the gene for a halophilic alkaline serine protease (halolysin) from an unidentified halophilic archaea strain (172P1) and expression of the gene in *Haloferax volcanii*. *J. Bacteriol.* 174, 736–742. doi: 10.1128/jb.174.3.736-742.1992

Karan, R., Capes, M. D., DasSarma, P., and DasSarma, S. (2013). Cloning, overexpression, purification, and characterization of a polyextremophilic β-galactosidase from the Antarctic haloarchaeon *Halorubrum lacusprofundi*. *BMC Biotechnol.* 13, 3. doi: 10.1186/1472-6750-13-3

Kim, J. S., Kluskens, L. D., de Vos, W. M., Huber, R., and van der Oost, J. (2004). Crystal structure of fervidolysin from *Fervidobacterium pennivorans*, a keratinolytic enzyme related to subtilisin. *J. Mol. Biol.* 335, 787–797. doi: 10.1016/j.jmb.2003.11.006

King, J., and Laemmli, U. K. (1971). Polypeptides of the tail fibres of bacteriophage T4. *J. Mol. Biol.* 62, 465–477. doi: 10.1016/0022-2836(71)90148-3

Kon, K., Shimanaga, M., and Horinouchi, M. (2020). "Marine ecology: Intertidal/Littoral zone," in *Japanese Marine life*. Eds. K. Inaba and J. Hall-Spencer (Singapore: Springer), 241–254. doi: 10.1007/978-981-15-1326-8_20

Lee, H. S. (2013). Diversity of halophilic archaea in fermented foods and human intestines and their application. *J. Microb. Biotechn.* 23, 1645–1653. doi: 10.4014/jmb.1308.08015

Lefebvre, O., and Moletta, R. (2006). Treatment of organic pollution in industrial saline wastewater: a literature review. *Water Res.* 40, 3671–3682. doi: 10.1016/j.watres.2006.08.027

Liu, G. M., Hou, J., Cai, S. F., Zhao, D. H., Cai, L., Han, J., et al. (2015). A patatin-like protein associated with the polyhydroxyalkanoate (PHA) granules of *Haloferax mediterranei* acts as an efficient depolymerase in the degradation of native PHA. *Appl. Environ. Microb.* 81, 3029–3038. doi: 10.1128/AEM.04269-14

Marem, A., Okamoto, D. N., Oliveira, L. C., Ruiz, D. M., Paggi, R. A., Kondo, M. Y., et al. (2018). Functional roles of c-terminal extension (CTE) of salt-dependent peptidase activity of the *Natrialba magadii* extracellular protease (NEP). *Int. J. Biol. Macromol.* 113, 1134–1141. doi: 10.1016/j.ijbiomac.2018.03.026

Quevillon, E., Silventoinen, V., Pillai, S., Harte, N., Mulder, N., Apweiler, R., et al. (2005). InterProScan: protein domains identifier. *Nucleic Acids Res.* 33, W116–W120. doi: 10.1093/nar/gki442

Ruiz, D. M., Iannuci, N. B., Cascone, O., and De Castro, R. E. (2010). Peptide synthesis catalysed by a haloalkaliphilic serine protease from the archaeon *Natrialba magadii* (Nep). *Lett. Appl. Microbiol.* 51, 691–696. doi: 10.1111/j.1472-765X.2010.02955.x

Ruiz, D. M., Paggi, R. A., Giménez, M. I., and De Castro, R. E. (2012). Autocatalytic maturation of the tat-dependent halophilic subtilase nep produced by the archaeon *Natrialba magadii. J. Bacteriol.* 194, 3700–3707. doi: 10.1128/JB.06792-11

Ryu, K., Kim, J., and Dordick, J. S. (1994). Catalytic properties and potential of an extracellular protease from an extreme halophile. *Enzyme Microb. Tech.* 16, 266–275. doi: 10.1016/0141-0229(94)90165-1

Shevchenko, A., Wilm, M., Vorm, O., and Mann, M. (1996). Mass spectrometric sequencing of proteins from silver-stained polyacrylamide gels. *Anal. Chem.* 68, 850–858. doi: 10.1021/ac950914h

Shi, W. L., Tang, X. F., Huang, Y. P., Gan, F., Tang, B., and Shen, P. (2006). An extracellular halophilic protease SptA from a halophilic archaeon *Natrinema* sp. J7: gene cloning, expression and characterization. *Extremophiles* 10, 599–606. doi: 10.1007/s00792-006-0003-8

Stroud, A., Liddell, S., and Allers, T. (2012). Genetic and biochemical identification of a novel single-stranded DNA-binding complex in *Haloferax volcanii. Front. Microbiol.* 3. doi: 10.3389/fmicb.2012.00224

Studdert, C. A., De Castro, R. E., Seitz, K. H., and Sánchez, J. J. (1997). Detection and preliminary characterization of extracellular proteolytic activities of the haloalkaliphilic archaeon *Natronococcus occultus. Arch. Microbiol.* 168, 532–535. doi: 10.1007/s002030050532

Studdert, C. A., Herrera Seitz, M. K., Plasencia Gil, M. I., Sanchez, J. J., and De Castro, R. E. (2001). Purification and biochemical characterization of the haloalkaliphilic archaeon *Natronococcus occultus* extracellular serine protease. *J. Basic Microb.* 41, 375–383. doi: 10.1002/1521-4028(200112)41:6<375::AID-JOBM375>3.0.CO;2-0

Sun, Y. P., Wang, B. B., Wu, Z. P., Zheng, X. W., Hou, J., and Cui, H. L. (2023). *Halorarius litoreus* gen. nov., sp. nov., *Halorarius halobius* sp. nov., *Haloglomus halophilum* sp. nov., *Haloglomus salinum* sp. nov., and *Natronomonas marina* sp. nov., extremely halophilic archaea isolated from tidal flat and marine solar salt. *Front. Mar. Sci.* 10. doi: 10.3389/fmars.2023.1105929

Vidyasagar, M., Prakash, S., Litchfield, C., and Sreeramulu, K. (2006). Purification and characterization of a thermostable, haloalkaliphilic extracellular serine protease from the extreme halophilic archaeon *Halogeometricum borinquense* strain TSS101. *Archaea* 2, 51–57. doi: 10.1155/2006/430763

Wang, Y. K., Zhao, G. Y., Li, Y., Chen, X. L., Xie, B. B., Su, H. N., et al. (2010). Mechanistic insight into the function of the c-terminal PKD domain of the collagenolytic serine protease deseasin MCP-01 from deep sea *Pseudoalteromonas* sp. SM9913: binding of the PKD domain to collagen results in collagen swelling but does not unwind the collagen triple helix. *J. Biol. Chem.* 285, 14285–14291. doi: 10.1074/jbc.M109.087023

Xu, Z. S., Du, X., Li, T.-T., Gan, F., Tang, B., and Tang, X. F. (2011). Functional insight into the c-terminal extension of halolysin SptA from haloarchaeon *Natrinema* sp. J7. *PloS One* 6, e23562. doi: 10.1371/journal.pone.0023562

Yongsawatdigul, J., Rodtong, S., and Raksakulthai, N. (2007). Acceleration of Thai fish sauce fermentation using proteinases and bacterial starter cultures. *J. Food Sci.* 72, M382–M390. doi: 10.1111/j.1750-3841.2007.00532.x

Zhang, Y. X., Wang, M. X., Du, X., Tang, W., Zhang, L., Li, M. R., et al. (2014). Chitin accelerates activation of a novel haloarchaeal serine protease that deproteinizes chitin-containing biomass. *Appl. Environ. Microb.* 80, 5698–5708. doi: 10.1128/AEM.01196-14